


REGULAR ARTICLE

Electron Transport Layer Material Optimization for Cs<sub>2</sub>AgBiBr<sub>6</sub>  
Based Solar Cell Using SCAPS

Sanat Das<sup>1</sup>, Prakash Babu Kanakavalli<sup>2</sup>, Sreevardhan Cheerla<sup>3</sup>, Sujubili Narzary<sup>1</sup>, Priyanko Protim Gohain<sup>1</sup>, Kunal Chakraborty<sup>1</sup>, Samrat Paul<sup>1,\*</sup> 

<sup>1</sup> Advanced Materials Research and Energy Application Laboratory (AMREAL), Department of Energy Engineering, North-Eastern Hill University, Shillong-793022, Meghalaya, India

<sup>2</sup> Department of Mechanical Engineering, Velagapudi Ramakrishna Siddhartha Engineering College, Kanuru-520007, Andhra Pradesh, India

<sup>3</sup> Department of Electronics and Communication Engineering, Koneru Lakshmaiah Education Foundation Green Fields, Vaddeswaram-522302, Andhra Pradesh, India

(Received 15 January 2024; revised manuscript received 17 February 2024; published online 28 February 2024)

The toxicity and stability concerns of lead based perovskite solar cells have limited the commercialization. The lead-free Cesium based double perovskite could be a viable answer to these issues. In this present work a theoretical analysis of Cesium based double perovskite solar cell using Spiro-OMeTAD as hole transport layer and effect of different ETLs such as SnO<sub>2</sub>, ZnO-NR, TiO<sub>2</sub> and CdS has been studied. The optimized active layer thickness of 0.3 μm has been used and a device structure of FTO/ETLs/Cs<sub>2</sub>AgBiBr<sub>6</sub>/Spiro-OMeTAD/Cu was simulated. The Solar Cell Capacitance Simulator (SCAPS-1D) was used for one dimensional simulation and analysis. The maximum PCE of 5.62 % was found using SnO<sub>2</sub> as ETL. The device performance has been optimized by employing various ETLs and the most suitable ETL for this structure was found to be SnO<sub>2</sub>. The maximum quantum efficiency of 86.09 % has been found for SnO<sub>2</sub> electron transport layer. The simulation results obtained in this study are encouraging and will provide insightful guidance in replacing toxic Pb-based perovskite with eco-friendly inorganic perovskite solar cell.

**Keywords:** SCAPS-1D, Double perovskite, Solar cell, Photovoltaic, Optimization, Electron transport layer, Hole Transport Layer, Quantum Efficiency, PCE, FF.

DOI: [10.21272/jnep.16\(1\).01014](https://doi.org/10.21272/jnep.16(1).01014)

PACS numbers: 73.50.Pz, 88.40.jp

## 1. INTRODUCTION

The rapid utilization of fossil fuels has drawn attention to alternative energy resources. Out of many available renewable energy sources, solar energy is the most promising and widely preferred [1-5]. In the recent past, organic-inorganic metal halide perovskite solar cells have been explored as an alternative to silicon-based solar cells for improving efficiency and are also preferred because of low manufacturing cost [6-10]. Lead (Pb) halide perovskites have excellent optoelectronic properties but the toxicity of Pb and poor stability are the principal reasons for not being suitable for commercial applications [11-16]. Lead-free double perovskites such as Cs<sub>2</sub>AgBiBr<sub>6</sub> have attractive optical and electronic properties. In this work, fully inorganic Cs<sub>2</sub>AgBiBr<sub>6</sub> as the absorber layer in the lead-free double perovskite solar cell (DPSC) *n-i-p* structure has been considered. Spiro-OMeTAD was employed as the hole transport layer. Fluorine-doped tin oxide and copper were employed as the front and back contact respectively. The DPSC structure FTO/ETLs/Cs<sub>2</sub>AgBiBr<sub>6</sub>/Spiro-OMeTAD/Cu was optimized by applying the various ETLs. The optimized thickness of the absorber layer was used. All these simulations were performed using SCAPS-1D.

The main purpose of this present work is to find an

efficient and lead-free double perovskite solar cell, by considering different ETLs. The most suitable ETL for the proposed device structure has been found without doing any experimental efforts which takes a lot of resources.

## 2. METHODOLOGY AND DEVICE ARCHITECTURE

The theoretical study of the device helps us in understanding the device mechanism without actual fabrication. It also gives an outline of the performance of the device. To study the solar cell device theoretically, SCAPS-1D solar cell simulation program for the simulation of the proposed device has been used. This software was developed by University of Gent, Belgium in 2000 and is freely available now [16-19]. The SCAPS program facilitates the modeling of planar as well as graded device structures up to seven layers and it has also the capability of computing the band alignment diagram, current-voltage characteristics, quantum efficiency, recombination and generation currents and other important parameters of the device. The SCAPS-1D is a one dimensional solar cell simulation program based on three coupled differential equations, namely Poisson's equation, the continuity equation for the electrons and the continuity equation for holes as follows:

\* Correspondence e-mail: [paulsamrat17@gmail.com](mailto:paulsamrat17@gmail.com)



$$\frac{d}{dx} \left( -\varepsilon(x) \frac{d\Psi}{dx} \right) = \quad (1)$$

$$= q \left[ p(x) - n(x) + N_d^+(x) - N_a^-(x) + p_t(x) - n_t(x) \right]$$

$$\frac{dp_n}{dt} = G_p - \frac{p_n - p_{n0}}{\tau_p} - \quad (2)$$

$$-p_n \mu_p \frac{d\xi}{dx} - \mu_p \xi \frac{dp_n}{dx} + D_p \frac{d^2 p_n}{dx^2}$$

$$\frac{dn_p}{dt} = G_n - \frac{n_p - n_{p0}}{\tau_n} + n_p \mu_n \frac{d\xi}{dx} \quad (3)$$

$$+ \mu_n \xi \frac{dn_p}{dx} + D_n \frac{d^2 n_p}{dx^2}$$

Here,  $D$  is diffusion coefficient,  $\Psi$  is electronic potential,  $q$  is electron charge,  $G$  is generation rate,  $\xi$  is permittivity, and  $n$ ,  $p$ ,  $n_t$ , and  $p_t$  are free holes, free electrons, trapped holes, and trapped electrons, respectively.  $N_a^-$  refers to ionized acceptor like doping concentration, and  $N_d^+$  stands for ionized donor-like doping concentration.



**Fig. 1** – Device structure used for simulation

In the present work, a conventional planar  $n-i-p$  device structure with lead free fully inorganic double perovskite  $\text{Cs}_2\text{AgBiBr}_6$  as the absorber layer, Spiro-OMeTAD as the hole transport layer, different ETLs ( $\text{SnO}_2$ ,  $\text{TiO}_2$ ,  $\text{ZnO-NR}$  and  $\text{CdS}$ ), fluorine doped tin oxide (FTO) and copper (Cu) as the front and back contacts respectively has been studied. The schematic of the device structure FTO/ETLs/ $\text{Cs}_2\text{AgBiBr}_6$ /Spiro-OMeTAD/Cu has been shown in Fig. 1.

The physical parameters of the material like band gap ( $E_g$ ), electron affinity ( $\chi$ ), dielectric permittivity ( $\varepsilon$ ), conduction and valence band density of state ( $N_c$  and  $N_v$ ), electron and hole thermal velocities ( $v_e$  and  $v_h$ ), acceptor and donor density ( $N_A$  and  $N_D$ ) and defect density ( $N_t$ ) are employed as the input parameters for the device simulation. These all parameters have been taken from the theoretical and experimental reported works and are given in Table 1 and 2 [16-22].

**Table 1** – SCAPS 1-D input material parameters used in the solar cell simulation for FTO, HTL and  $\text{Cs}_2\text{AgBiBr}_6$

Parameters	Window Layer FTO	HTL Spiro-OMeTAD	Absorber Layer $\text{Cs}_2\text{AgBiBr}_6$
Thickness, $\mu\text{m}$	0.2	0.3	0.1-1
Bandgap ( $E_g$ ), eV	3.2	3.0	2.05
Electron affinity ( $\chi$ ), eV	4.4	2.45	4.19
Relative Permittivity ( $\varepsilon_r$ )	9.0	3.0	5.80
CB effective density of states ( $N_c$ ), $\text{cm}^{-3}$	2.2E+18	2.2E+19	1.0E+16

VB effective density of states ( $N_v$ ), $\text{cm}^{-3}$	1.8E+19	1.8E+19	1.0E+16
Electron mobility ( $\mu_n$ ), $\text{cm}^2 \cdot \text{V}^{-1} \cdot \text{s}^{-1}$	20	2.0E-4	11.81
Hole mobility ( $\mu_p$ ), $\text{cm}^2 \cdot \text{V}^{-1} \cdot \text{s}^{-1}$	10	2.0E-4	0.49
Donor density ( $N_D$ ), $\text{cm}^{-3}$	1.0E+18	0	1.0E+19
Acceptor density ( $N_A$ ), $\text{cm}^{-3}$	0	1.0E+18	1.0E+19
Defect Density ( $N_t$ ), $\text{cm}^{-3}$	1.0E+15	1.0E+14	9.1E+16

The values of parameters not included in the table are set identical for all layers. Neutral Gaussian distribution defect is adopted with characteristic energy being set to 0.1 eV. The electron and hole capture cross section is set to  $9 \times 10^{-15} \text{ cm}^2$  with the thermal velocity of both carriers fixed at  $10^7 \text{ cm/s}$ . The ETL plays an important role in the device to extract the electrons from the perovskite layer and block the recombination between electrons in the FTO and holes in the perovskite layer [23-26]. Till now,  $\text{TiO}_2$  has been used as an ETL in most reported PSCs.  $\text{TiO}_2$  ETLs were widely applied in dye-sensitized solar cells. The conduction band maximum (CBM) and valence band maximum (VBM) of  $\text{TiO}_2$  are  $-4.4 \text{ eV}$  and  $-7.63 \text{ eV}$  respectively which guarantee not only efficient electron transport from the perovskite layer but efficient hole-blocking ability at the perovskite interface. The thickness and contact optimization of the ETL is very important to get maximum efficiency. But too thick ETL can minimize the recombination in the device and the electron flow may be hampered due to high resistance. Thus, contact between FTO and ETL should be considered carefully [12-16].

**Table 2** – SCAPS 1-D input material parameters used in the solar cell simulation for different ETL materials

Parameter	ETL1 $\text{SnO}_2$	ETL2 $\text{TiO}_2$	ETL3 $\text{ZnO-NR}$	ETL4 $\text{CdS}$
Thickness, $\mu\text{m}$	0.3	0.3	0.3	0.3
Bandgap ( $E_g$ ), eV	3.6	3.2	3.47	2.4
Electron affinity ( $\chi$ ), eV	4.4	4.1	4.3	4.18
Relative Permittivity ( $\varepsilon_r$ )	9	9.0	9	10
CB effective density of states ( $N_c$ ), $\text{cm}^{-3}$	2.2E+18	2.2E+18	2E+18	2.2E+18
VB effective density of states ( $N_v$ ), $\text{cm}^{-3}$	1.8E+19	1E+19	1.8E+20	1.9E+19
Electron mobility ( $\mu_n$ ), $\text{cm}^2 \cdot \text{V}^{-1} \cdot \text{s}^{-1}$	100	20	1E+2	100
Hole mobility ( $\mu_p$ ), $\text{cm}^2 \cdot \text{V}^{-1} \cdot \text{s}^{-1}$	2.56E-1	10	2.5E+1	25
Donor density ( $N_D$ ), $\text{cm}^{-3}$	1E+17	1E+18	1E+19	1E+18
Acceptor density ( $N_A$ ), $\text{cm}^{-3}$	0	0	0	0
Defect Density ( $N_t$ ), $\text{cm}^{-3}$	1E+15	1E+15	1E+18	1E+15

### 3. RESULTS AND DISCUSSION

In this work,  $\text{SnO}_2$ ,  $\text{TiO}_2$ ,  $\text{ZnO-NR}$  and  $\text{CdS}$  have been used as the ETL layer for the simulation of double perovskite solar cell (DPSC). The energy band alignment diagram for various ETLs is shown in Fig. 2. All the ETL materials used in this work have been inspected along with Spiro-OMeTAD,  $\text{Cu}_2\text{O}$  and  $\text{CuSCN}$  as the HTL layer of  $\text{CH}_3\text{NH}_3\text{PbI}_3$  based PSCs in various publications. However, this work focuses on to promote a lead free double perovskite solar cell structure with Spiro-OMeTAD as the HTL. Along with the  $I$ - $V$  characteristics, effect of some fundamental parameters such as band gap, electron affinity, dielectric permittivity, electron affinity, dielectric per-

mittivity, electron and hole mobility has also been observed using different ETL layers. The optimum values of parameters are based on reported literatures [5-10] which are summarized in Table 2.

Fig. 3 shows the  $J$ - $V$  curves for DPSCs having  $\text{SnO}_2$ ,  $\text{TiO}_2$ ,  $\text{ZnO-NR}$  and  $\text{CdS}$  as the ETL layers. The optimized thickness of  $0.3 \mu\text{m}$  of the perovskite layer has been considered. Table 3 shows the performance of lead-free double perovskite solar cell with different ETL layers.

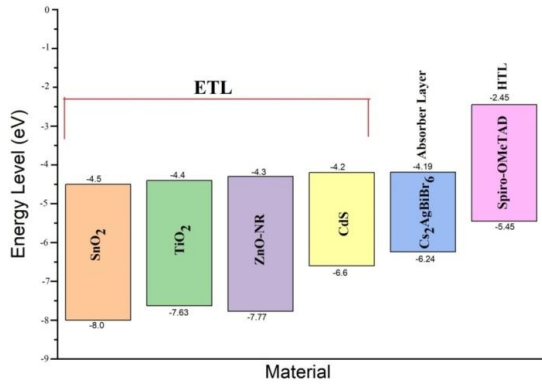


Fig. 2 – Energy Band Alignment

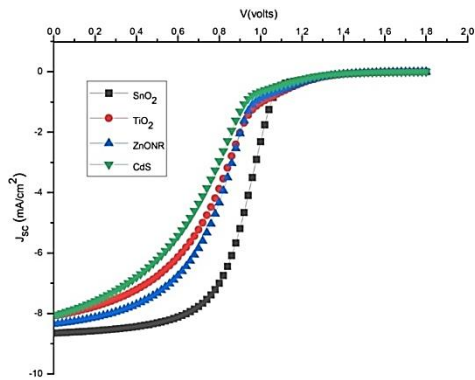


Fig. 3 –  $J$ - $V$  curves for different ETLs

It can clearly be observed from Table 3 that the DPSC has the best performance when  $\text{SnO}_2$  has been used as the ETL layer.  $\text{SnO}_2$  gives the highest values of PCE of 5.62 %,  $J_{sc}$  of 8.648  $\text{mA}/\text{cm}^2$  and also FF of 36.38 %. Therefore,  $\text{SnO}_2$  has been selected as the ETL, with optimal absorber layer thickness of  $0.3 \mu\text{m}$ . The reason for this better PCE of  $\text{SnO}_2$  can be elicited from Fig. 2 i.e energy band diagram. In Fig. 2, the conduction band offset (CBO) is negative for all ETLs. When CBO is negative,  $V_{oc}$  decreases monotonically. The negative CBO being very small there is no effect on the value of  $V_{oc}$  and FF [14]. According to literature, all the ETLs have a good band alignment with the current absorber layer. So a constant  $J_{sc}$  for all ETLs should have been obtained. But the  $J_{sc}$  of 8.648  $\text{mA}/\text{cm}^2$  for  $\text{SnO}_2$ , 8.354  $\text{mA}/\text{cm}^2$  for  $\text{ZnO-NR}$ , 8.085  $\text{mA}/\text{cm}^2$  for  $\text{TiO}_2$  and 8.068  $\text{mA}/\text{cm}^2$  for  $\text{CdS}$  has been obtained due to the variation in its quantum efficiency ( $QE$ ) which is shown in Fig. 4. As  $J_{sc}$  varies, the PCE of structure using different ETLs also varies.

From Fig. 4, It has been found that the  $\text{SnO}_2$ ,  $\text{ZnO-NR}$ ,  $\text{TiO}_2$  and  $\text{CdS}$  exhibit as much as 86.09 %, 84.4 %, 80.46 % and 76.01 %  $QE$  respectively at around 390 nm wavelengths. The Table 4 summarizes the maximum  $QE$  at 390

nm wavelength. Therefore, the  $\text{SnO}_2$  as the ETL has been selected for the proposed DPSC having highest PCE of 5.62 % and  $QE$  of 86.09 % among all the tested ETLs.

Table 3 – Performance of DPSC with different ETL layers

ETL layer	$V_{oc}$ (Volts)	$J_{sc}$ ( $\text{mA}/\text{cm}^2$ )	FF (%)	PCE (%)
$\text{SnO}_2$	1.787	8.648	36.38	5.62
$\text{ZnO-NR}$	1.871	8.354	26.41	4.13
$\text{TiO}_2$	1.835	8.085	25.07	3.72
$\text{CdS}$	1.830	8.068	22.04	3.26

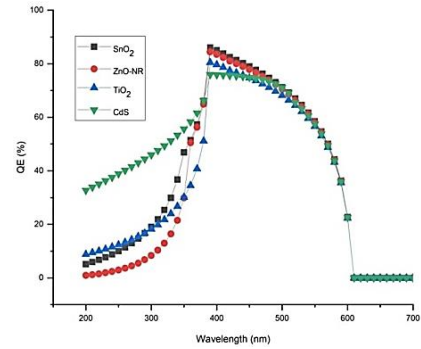


Fig. 4 – Quantum Efficiency curves for various ETLs at optimal absorber layer thickness

Table 4 – Maximum Quantum Efficiency at 390 nm Wavelength

ETL (Electron Transport Layer)	Maximum QE (%) at 390 nm wavelength
$\text{SnO}_2$	86.09
$\text{ZnO-NR}$	84.40
$\text{TiO}_2$	80.46
$\text{CdS}$	76.01

### Comparison of Reported Perovskite Structure with Recently Reported Results

There are scanty literatures for the present DPSC for a better comparison of the present results. However, some of the recently published literatures have used Pb (lead) based perovskite which is toxic in nature [19], as compared to present device structure which is a lead-free double perovskite structure. The reported results of Bhavsar et al. [19] and Hongsith et al. [20] shown in Table 5 have used organic structure which is unstable compared to the reported perovskite material under study. Moreover, the device architecture studied is not the complete device architecture and hence, the results may not be comparable.

Table 5 – Comparison of PCE with recently reported literature

Device Structure	PCE (%)
FTO/ $\text{SnO}_2$ / $\text{Cs}_2\text{AgBiBr}_6$ /Spiro-OMeTAD/Cu (Present Work)	5.62 (Present work)
$\text{ZnO}/\text{MAPbI}_3$ /Spiro-OMeTAD [19]	21.73
Ag/Spiro-OMeTAD/Perovskite/ $\text{SnO}_2$ / $\text{SnO}_x$ [20]	18.39
ITO/PEDOT:PSS/ $\text{CsSnI}_3$ / $\text{ZnONP}/\text{Ag}$ [22]	6.08

## 4. CONCLUSION

The simulations of lead-free double perovskite  $\text{Cs}_2\text{AgBiBr}_6$  based solar cell having Spiro-OMeTAD as the hole transport layer and different ETL materials have been used. From the simulations, it has been deduced that  $J$ - $V$  characteristics of the DPSC model have indicated high-efficiency performance. Among all the ETL layers, the best performance has been achieved for the lead free DPSC having  $\text{SnO}_2$  as ETL ( $J_{sc} = 8.648 \text{ mA}/\text{cm}^2$ ,  $V_{oc} = 1.787 \text{ Volts}$ , FF = 36.38 %, PCE = 5.62 %,

QE = 86.09 %). For the justification of the proposed model, simulation has been done for lead free DPSC structure using SCAPS-1D. Simulations have been done to analyze the effects of electrical parameters on lead free double perovskite  $\text{Cs}_2\text{AgBiBr}_6$  based solar cell. From the results of the simulations, it can be summarized that FTO/ $\text{SnO}_2$ / $\text{Cs}_2\text{AgBiBr}_6$ /Spiro-OMeTAD/Cu lead free DPSC structure is a potential alternative for solar cell which can be reasonably efficient and inexpensive.

## REFERENCES

1. A.K. Das, R. Mandal, D. Mandal, *Opt. Quant. Electron.* **54**, 455 (2022).
2. S. Abdelaziz, A. Zekry, A. Shaker, M. Abouelatta, *Opt. Mat.* **123**, 111893 (2022).
3. H. Sabbah, *Materials* **15**, 3229 (2022).
4. S. Das, M.G. Choudhury, S. Paul, *J. Nano- Electron. Phys.* **14** No 3, 03012 (2022).
5. S.A. Moiz, *Photonics* **9**, 23 (2022).
6. A. Tara, V. Bharti, S. Sharma, R. Gupta, *Opt. Mat.* **119**, 111362 (2021).
7. I. Jeon, K. Kim, E. Jokar, M. Park, H.W. Lee, E.W.G. Diao, *Nanomaterials* **11**, 2066 (2021).
8. R.T. Mouchou, T.C. Jen, O.T. Laseinde, K.O. Ukoba, *Mater. Today Proc.* **38**, 835 (2021).
9. D. Rached, W.L. Rahal, *Optik* **223**, 165575 (2020).
10. N. Singh, A. Agarwal, M. Agarwal, *Opt. Mat.* **114**, 110964 (2021).
11. S. Das, K. Chakraborty, M.G. Choudhury, S. Paul, *J. Nano- Electron. Phys.* **13** No 3, 03018 (2021).
12. N. Aste, C. Del Pero, F. Leonforte, *Sol. Energy* **109**, 1 (2014).
13. M. Abderrezek, M.E. Djeghlal, *Optik* **242**, 167320 (2021).
14. A. Sunny, S. Rahman, Most. Marzia Khatun, Sheikh Rashel Al Ahmed, *AIP Adv.* **11**, 065102 (2021).
15. M. Salem, A. Shaker et al., *Energies* **14**, 5741 (2021).
16. S.S. Hussain, S. Riaz et al., *J. Renew. Energy* **2021**, 6668687 (2021).
17. M.A. Green, E.D. Dunlop, D.H. Levi, J. Hohl-Ebinger, M. Yoshita, A.W.Y. Ho-Baillie, *Prog. Photovolt.: Res. Appl.* **27**, 565 (2019).
18. M.K. Mottakin et al., *Energies* **14**, 7200 (2021).
19. K. Bhavsar, P. Lapsiwala, *Semiconductor Physics, Quantum Electronics & Optoelectronics* **24**, 341 (2021).
20. T. Ishii, K. Otani, T. Takashima, S. Kawai, *Sol. Energy Mater. Sol. C.* **95**, 386 (2011).
21. A. Kanevce, W.K. Metzger, *J. Appl. Phys.* **105** No 9, 094507 (2009).
22. S. Ma, X. Gu, *ACS Appl. Mater. Interface.* **4** (2021).
23. H. Shao, N.H. Ladi, *Solar RRL* **5** (2021).
24. K. De Cock, S. Khelifi, M. Burgelman, *Thin Solid Films* **519**, 7481 (2011).
25. L. Zhao, C.L. Zhou, H.L. Li, H.W. Diao, W.J. Wang, *Sol. Energy Mater. Sol. C.* **92**, 673 (2008).
26. J. Madan, R. Pandey, R. Sharma, *Solar Eng.* **197**, 212 (2020).

## ACKNOWLEDGEMENTS

The authors are thankful to Prof. Marc Burgelman, University of Gent, Belgium for providing the SCAPS 1-D software for our studies. The authors are also thankful to the Science and Engineering Research Board (SERB), Department of Science and Technology (DST) India for their financial support (EMR/2016/002430) to carry out this research work.

## Оптимізація матеріалу електронного транспортного шару для $\text{Cs}_2\text{AgBiBr}_6$ на основі сонячної батареї з використанням SCAPS

Sanat Das<sup>1</sup>, Prakash Babu Kanakavalli<sup>2</sup>, Sreevardhan Cheerla<sup>3</sup>, Sujubili Narzary<sup>1</sup>, Priyanko Protim Gohain<sup>1</sup>, Kunal Chakraborty<sup>1</sup>, Samrat Paul<sup>1</sup>

<sup>1</sup> *Advanced Materials Research and Energy Application Laboratory (AMREAL), Department of Energy Engineering, North-Eastern Hill University, Shillong-793022, Meghalaya, India*

<sup>2</sup> *Department of Mechanical Engineering, Velagapudi Ramakrishna Siddhartha Engineering College, Kanuru-520007, Andhra Pradesh, India*

<sup>3</sup> *Department of Electronics and Communication Engineering, Koneru Lakshmaiah Education Foundation Green Fields, Vaddeswaram-522302, Andhra Pradesh, India*

Проблеми з токсичністю та стабільністю перовскітних сонячних батарей на основі свинцю обмежили комерціалізацію. Подвійний перовскіт на основі цезію, що не містить свинцю, може стати життєздатною відповіддю на ці проблеми. У цій роботі проведено теоретичний аналіз подвійної перовскітної сонячної батареї на основі цезію з використанням Spiro-OMeTAD як шару для транспортування дірок і ефекту різних ETL, таких як  $\text{SnO}_2$ ,  $\text{ZnO-NR}$ ,  $\text{TiO}_2$  і  $\text{CdS}$ . Було використано оптимізовану товщину активного шару 0,3 нм і змодельовано структуру пристрою FTO/ETLs/ $\text{Cs}_2\text{AgBiBr}_6$ /Spiro-OMeTAD/Cu. Симулятор емності сонячних батарей (SCAPS-1D) використовувався для одновимірного моделювання та аналізу. Максимальний PCE 5,62 % було знайдено з використанням  $\text{SnO}_2$  як ETL. Продуктивність пристрою була оптимізована шляхом використання різних ETL, і було виявлено, що найбільш підходящим ETL для цієї структури є  $\text{SnO}_2$ . Максимальна квантова ефективність 86,09 % отримана для електронотранспортного шару  $\text{SnO}_2$ . Результати моделювання перспективні та дадуть глибокі вказівки щодо заміни токсичного перовскіту на основі свинцю екологічно чистими сонячними елементами з неорганічного перовскіту.

**Ключові слова:** SCAPS-1D, Подвійний перовскіт, Сонячна батарея, Оптимізація, Електротранспортний шар, Квантова ефективність, PCE, FF.